

The effect of ring size variation on the structure and stability of lanthanide(III) complexes with crown ethers containing picolinate pendants[†]

Adrián Roca-Sabio, Marta Mato-Iglesias, David Esteban-Gómez, Andrés de Blas, Teresa Rodríguez-Blas and Carlos Platas-Iglesias

Departamento de Química Fundamental, Universidade da Coruña, Campus da Zapateira-Rúa da Fraga 10, 15008 A, Coruña, Spain

Dalton Transactions Volume 40, Issue 2, pages 384–392, 14 January 2011

Received 29 June 2010, Accepted 06 October 2010, First published 29 November 2010

How to cite:

The effect of ring size variation on the structure and stability of lanthanide(III) complexes with crown ethers containing picolinate pendants. A. Roca-Sabio, M. Mato-Iglesias, D. Esteban-Gómez, A. de Blas, T. Rodríguez-Blas and C. Platas-Iglesias, *Dalt. Trans.*, 2011, **40**, 384–392. DOI: [10.1039/C0DT00746C](https://doi.org/10.1039/C0DT00746C).

Abstract

The coordination properties of the macrocyclic receptor *N,N'*-bis[(6-carboxy-2-pyridyl)methylene]-1,10-diaza-15-crown-5 ($H_2bp15c5$) towards the lanthanide ions are reported. Thermodynamic stability constants were determined by pH-potentiometric titration at 25 °C in 0.1 M KCl. A smooth decrease in complex stability is observed upon decreasing the ionic radius of the Ln^{III} ion from La [$\log K_{LaL} = 12.52(2)$] to Lu [$\log K_{LuL} = 10.03(6)$]. Luminescence lifetime measurements recorded on solutions of the Eu^{III} and Tb^{III} complexes confirm the absence of inner-sphere water molecules in these complexes. 1H and ^{13}C NMR spectra of the complexes formed with the diamagnetic La^{III} metal ion were obtained in D_2O solution and assigned with the aid of HSQC and HMBC 2D heteronuclear experiments, as well as standard 2D homonuclear COSY and NOESY spectra. The 1H NMR spectra of the paramagnetic Ce^{III} , Eu^{III} and Yb^{III} complex suggest nonadentate binding of the ligand to the metal ion. The *syn* conformation of the ligand in $[Ln(bp15c5)]^+$ complexes implies the occurrence of two helicities, one associated with the layout of the picolinate pendant arms (absolute configuration Δ or Λ), and the other to the five five-membered chelate rings formed by the binding of the crown moiety (absolute configuration δ or λ). A detailed conformational analysis performed with the aid of DFT calculations (B3LYP model) indicates that the complexes adopt a $\Lambda(\lambda\delta)(\delta\delta\lambda)$ [or $\Delta(\delta\lambda)(\lambda\lambda\delta)$] conformation in aqueous solution. Our calculations show that the interaction between the Ln^{III} ion and several donor atoms of the crown moiety is weakened as the ionic radius of the metal ion decreases, in line with the decrease of complex stability observed on proceeding to the right across the lanthanide series.

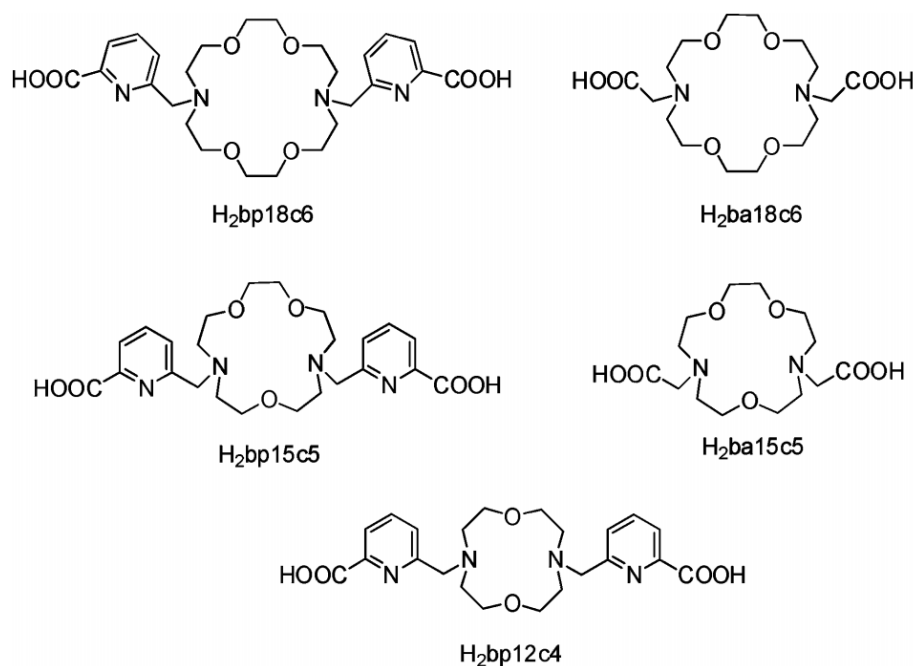
Keywords: picolinate ligands; crystal structures; lanthanide complexes; crown ethers; stability in solution

Introduction

The lanthanides constitute an unique series of elements characterized by the common +III oxidation state and the so called lanthanide contraction, the small monotonous contraction of the ionic radius upon increasing atomic number.¹ However, the overall relative contraction of ionic radius on going from La^{III} (1.216 Å for CN 9) to Lu^{III} (1.031 Å for CN 9) amounts only to *ca.* 15%.² As a consequence, the Ln^{III} ions possess similar physical and chemical properties, the separation of lanthanides into individual elements being rather

difficult.³ Thus, the design of systems that can selectively recognize a given Ln^{III} ion, or at least a particular group of them, remains a challenging task for coordination chemistry.⁴ As far as coordination chemistry in aqueous solution is concerned, the Ln^{III} ions are dominated by their oxophilicity,⁵ as well as by their tendency to adopt high coordination numbers (typically 8 or 9).⁶ As a result, stable Ln^{III} complexation in aqueous solution is normally achieved by using octa- or nona-dentate ligands containing negatively charged oxygen donors such as carboxylates or phosphonates.⁷ Besides negatively charged oxygen groups, these ligands often contain N-donor atoms such as amine or pyridine nitrogen atoms that contribute to form stable complexes in aqueous solutions. For instance, several macrocyclic receptors containing pyridine units either within the macrocyclic framework⁸ or as pendant arms⁹ have been shown to provide stable Ln^{III} complexation in water. Furthermore, polydentate ligands containing picolinate groups also form stable complexes with the Ln^{III} ions in water.^{10,11}

The stability trends for Ln^{III} complexes in aqueous solution usually fall within one of the following categories: (i) In the most common case, the stability constants increase across the lanthanide series from La^{III} to Lu^{III}, as expected on the basis of the simple electrostatic interaction between the metal ion and the donor atoms of the ligand;¹² (ii) For a second group of ligands the stability of the corresponding Ln^{III} complexes increases across the series, reaches a plateau, and then declines;^{13,14} (iii) The third class of ligands includes a few macrocycles such as ba18c6 (Scheme 1), for which the stability decreases along the lanthanide series.¹⁵ However, independently of the stability trend, most of the ligands provide limited discrimination along the lanthanide series, except for a few cases where an important selectivity was found for the heavier lanthanides.¹⁶



Scheme 1. Ligands discussed in the present work.

Macrocyclic receptors such as crown ethers possess a high level of preorganization that often results in superior selectivities of their complexes with metal ions in comparison to those of acyclic ligands.^{17,18} Three major strategies emerge for achieving effective complexation of a particular metal ion with a macrocyclic ligand:^{19,20} (i) the use of donor set variation to tune the affinity of the receptor towards particular

metal ions; (ii) the use of ring size variation to maximize the thermodynamic stability of the complex by matching the radius of the metal ion and the hole size of the macrocyclic moiety (the hole-size effect); and (iii) the introduction of adequate pendant arms to improve the selectivity for a particular metal ion with respect to the parent macrocycle. The match between these structural properties of the ligand and the coordination properties of the metal ion usually determines the stability of the corresponding complex.

In a recent paper we reported the complexation properties towards the Ln^{III} ions of the macrocyclic receptor containing picolinate pendant arms bp18c6 (Scheme 1).²¹ This receptor shows an unprecedented selectivity for the large Ln^{III} ions. The La^{III} and Ce^{III} complexes show the highest log K_{ML} values among the different Ln^{III} ions, with a dramatic drop of the stability being observed from Ce^{III} to Lu^{III} as the ionic radius of the Ln^{III} ions decreases (log K_{CeL} – log K_{LuL} = 6.9). This drop in the log K_{ML} values is six orders of magnitude higher than that observed for ba18c6 (1.4). In the [Ln(bp18c6)]⁺ complexes the metal ion is directly bound to the ten donor atoms of the bp18c6 ligand, but the interaction between the Ln^{III} ion and several donor atoms of the crown moiety is weakened as the ionic radius of the metal ion decreases. Instead, the stability of the Ln^{III} complexes of bp12c4 increases across the lanthanide series, reaches a plateau close to the middle of the series, and then slightly decreases for the smallest lanthanides.²² In the [Ln(bp12c4)]⁺ complexes the metal ion is directly bound to the eight donor atoms of the ligand. The lower denticity of bp12c4 in comparison to bp18c6 allows the additional coordination of water molecules to the metal ions. Indeed, the hydration numbers obtained from luminescence lifetime measurements in aqueous solution of the Eu^{III} and Tb^{III} complexes suggest an equilibrium between a dihydrated ($q = 2$), ten-coordinate and a monohydrated ($q = 1$), nine-coordinate species.²³

As a continuation of our previous work, herein we report the complexation properties towards the Ln^{III} ions of the macrocyclic ligand *N,N'*-Bis[(6-carboxy-2-pyridyl)methylene]-1,10-diaza-15-crown-5 (H₂bp15c5, Scheme 1). The aim of this work is to evaluate the effect that macrocyclic ring size variation has on the stability and structure in solution of the Ln^{III} complexes with the series of ligands bp12c4, bp15c5 and bp18c6. Thermodynamic stability constants of the Ln^{III} complexes of bp15c5 have been determined by pH potentiometry. Aiming to rationalize the stability trend observed across the lanthanide series the structure of the Ln^{III} complexes was studied by using ¹H and ¹³C NMR techniques in D₂O solution. Luminescence lifetime measurements on the Eu^{III} and Tb^{III} complexes have been carried out to determine the hydration number of the complexes in solution. In addition, the complexes were characterized by density functional theory (DFT) calculations carried out at the B3LYP level.

Results and discussion

Ligand protonation constants and stability constants of the metal complexes

The protonation constants of bp15c5 as well as the stability constants of its metal complexes formed with Ca^{II} and several Ln^{III} ions were determined by potentiometric titration in 0.1 M KCl; the constants and standard deviations are given in Table 1, which also lists the protonation and stability constants reported for the related systems bp12c4,²² bp18c6,²¹ ba15c5²⁴ and ba18c6¹⁵ (Scheme 1). The protonation constants reported in Table 1 for bp15c5 (8.34, 6.85 and 3.05, $I = 0.1$ M KCl) differ significantly from the values measured at $I = 0.1$ M KNO₃ (8.21, 7.19, 3.43 and 2.53),²⁵ which most likely reflects a different ability of the two anions to bind protonated forms of the ligand.²⁶ The ligand protonation constants are defined as in eqn (1), and the stability constants of the metal complexes are expressed in eqn (2):

$$K_i = \frac{[H_iL]}{[H_{i-1}L][H^+]} \quad (1)$$

$$K_{ML} = \frac{[ML]}{[M][L]} \quad (2)$$

In comparison to the bisacetate derivative of the same macrocycle (ba15c5, Scheme 1), bp15c5 has lower protonation constants for the first and second protonation steps, which occur on the amine nitrogen atoms. This is in line with previous investigations, which showed that the replacement of the carboxylate groups of edta by pyridinecarboxylate units leads to a decrease in the basicity of the two amine nitrogen atoms.^{27,28} The basicity of the amine nitrogen atoms varies in the following order: bp12c4 > bp15c5 > bp18c6. Thus, the basicity of the pivotal nitrogen atoms decreases as the size of the crown moiety increases, in agreement with the trend observed for the bisacetate derivatives ba15c5 and ba18c6. The third protonation process in bp15c5 is attributed to the protonation of the pyridylcarboxylate groups.^{29,30}

Table 1. Ligand protonation constants and thermodynamic stability constants of bp15c5 and its metal complexes as determined by pH-potentiometry [$I = 0.1$ M KCl]. Data reported previously for related ligands are provided for comparison.

	bp15c5	bp12c4 ^a	bp18c6 ^b	ba15c5 ^c	ba18c6 ^d
log K_1	8.34(4)	9.16	7.41	9.02	8.45
log K_2	6.85(4)	7.54	6.85	8.79	7.80
log K_3	3.05(4)	3.76	3.32	2.95	2.90
log K_4		2.79	2.36		
log K_{LaL}	12.52(2)	16.81	14.99	10.11	12.21
log K_{CeL}	12.32(2)	16.94	15.11	10.89	12.23
log K_{EuL}	12.01(2)	18.62	13.01	11.85	12.02
log K_{GdL}	11.41(3)	18.82	13.02	11.66	11.93
log K_{DyL}	10.83(4)	18.11	11.72	11.55	11.57
log K_{YbL}	9.99(4)	18.08	8.89	10.76	10.90
log K_{LuL}	10.03(6)	^e	8.25	10.33	10.84
log K_{CaL}	7.54(8)	12.09	^e	8.74	8.39

a Ref. 22. *b* Ref. 21. *c* Ref. 24. *d* Ref. 15. *e* Not determined.

Potentiometric titrations of H₂bp15c5 have been carried out in the presence of equimolar Ln^{III} and Ca^{II} ions in order to determine the stability constants of the corresponding metal complexes (Table 1). The variation of the stability constants across the lanthanide series for the complexes of bp15c5 is compared to those of bp12c4 and bp18c6 in Fig. 1. The bp15c5 complex of La^{III} shows the highest log K_{ML} value among the different Ln^{III} ions, with a smooth drop of the stability being observed from La^{III} to Lu^{III} as the ionic radius of the Ln^{III} ions decreases. The opposite trend is observed for most classical polydentate acyclic and macrocyclic ligands in aqueous solution, whose stability constants with Ln^{III} ions increase from La^{III} to Lu^{III} due to the increasing charge density of the metal ions. The trend observed for bp15c5 is also different to that observed for ba15c5, for which the stability constants increase across the series for the large Ln^{III} ions, reach a maximum close to the centre of the series, and then decline (Table 1, Fig. 1). The stability constants observed for bp15c5 complexes follow a trend that is similar to that reported for bp18c6.²¹ However, the stability drop observed for bp15c5 complexes ($\Delta \log K_{ML} = \log K_{LaL} - \log K_{LuL} = 2.5$) is less important than that determined for the bp18c6 analogues ($\Delta \log K_{ML} = \log K_{LaL} - \log K_{LuL} = 6.7$). As a consequence, the

complexes of bp18c6 are more stable than the bp15c5 counterparts for the large Ln^{III} ions, while for the heaviest lanthanides the complexes of bp15c5 become slightly more stable than those derived from the large crown moiety. However, the ligand containing the smallest crown moiety fragment, bp12c4, forms complexes that are more stable than the bp15c5 and bp18c6 analogues along the whole lanthanide series (Fig. 1). It is rather obvious that among this series of ligands the 12-membered macrocyclic ring of bp12c4 provides the best fit with the Ln^{III} ions. The complexes of bp12c4 are more stable than the edta³⁻ counterparts for the large Ln^{III} ions, while this situation is reversed close to the end of the lanthanide series. This is a consequence of the different stability trends of edta and bp12c4 complexes along the series. Indeed, Ln^{III}-edta complexes represent a classical example for which the stability is increasing along the lanthanide series, while the bp12c4 counterparts show a stability trend similar to that observed for dtpa³⁻ complexes (Fig. 1). A comparison of the stability constants obtained for bp15c5 and bp18c6 complexes with those reported for the corresponding bisacetate derivatives shows that the replacement of the carboxylate groups of ba15c5 and ba18c6 by pyridinecarboxylate units leads to an increased stability of the complexes with the large Ln^{III} ions (see data for bp15c5 and ba15c5 in Fig. 1).

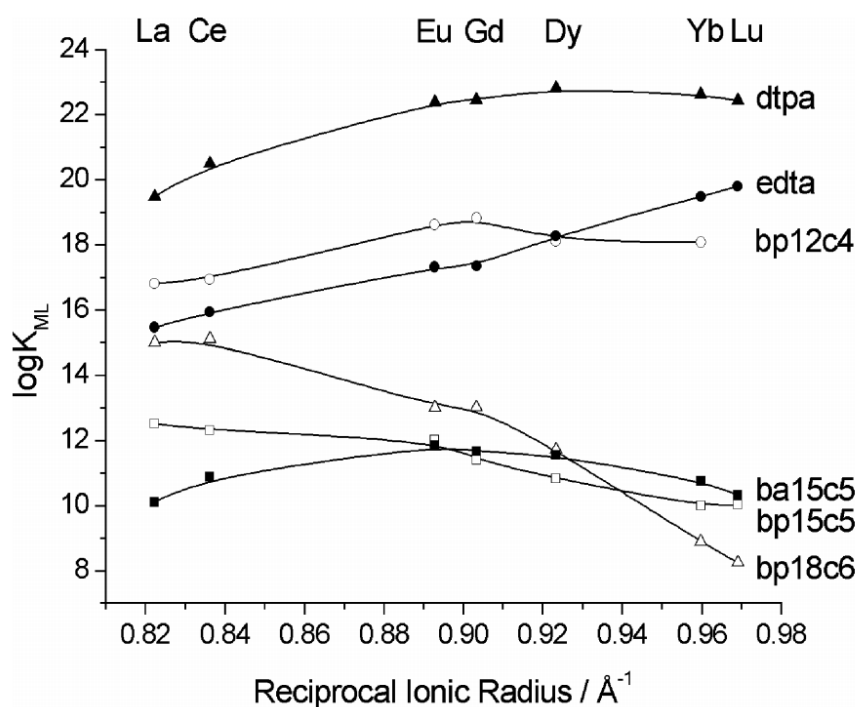


Fig. 1. Variation of the stability constants ($\log K_{ML}$ values, $I = 0.1$ M KCl, 25 °C) across the lanthanide series for bp15c5 complexes and related systems. The solid lines are simply a guide for the eye. Ionic radii were taken from reference 2 assuming coordination number 9.

Photophysical properties

The absorption spectra of the $[\text{Ln}(\text{bp15c5})]^+$ complexes (Ln = Eu or Tb) are dominated by a weak absorption band at *ca.* 273 nm typical of the picolinate chromophore (Fig. 2, see also Table 2).³³ The emission spectra of both complexes recorded under excitation through the ligand bands show the typical narrow transitions characteristic of the corresponding metal ion as a consequence of ligand-to-metal energy transfer.³⁴ In the case of the Eu^{III} complex the $^5D_0 \rightarrow ^7F_J$ transitions are observed around 580 ($J = 0$), 593 ($J = 1$), 612 ($J = 2$), 652 ($J = 3$) and 678 nm ($J = 4$). For the Tb^{III} analogue the typical $^5D_4 \rightarrow ^7F_J$ are observed around 623 ($J = 3$), 584 ($J = 4$), 545 ($J = 5$) and 490 nm ($J = 6$). Recording the excitation spectra with emission monitored on the

most intense emission band of the lanthanide cations ($^5D_0 \rightarrow ^7F_2$ at 612 nm for Eu^{III} and $^5D_4 \rightarrow ^7F_5$ at 545 nm for Tb^{III}) afforded a perfect match with the corresponding absorption spectra, thereby unambiguously confirming the antenna effect.³³ The absolute quantum yields of the metal centred luminescence amount to 0.13 (Eu^{III}) and 2.5% (Tb^{III}). These data show that picolinate units of bp15c5 allow relatively efficient sensitization of the Tb^{III} luminescence as a result of an efficient ligand-to-metal energy transfer and effective shielding of the metal ion from radiationless deactivation (see below). The quantum yield observed for the Eu^{III} complex is considerably lower than that determined for the Tb^{III} analogue, as usually observed for Ln^{III} complexes containing picolinate units.¹¹ The quantum yields determined for the Eu^{III} and Tb^{III} complexes of bp15c5 are however considerably lower than those reported for the corresponding *tri*(dipicolinates), which amount to 24% (Eu^{III}) and 22% (Tb^{III}).³⁵

Table 2. Spectroscopic properties of the Eu^{III} and Tb^{III} complexes of bp15c5.

	$[\text{Eu}(\text{bp15c5})]^+$	$[\text{Tb}(\text{bp15c5})]^+$
$\lambda_{\text{max}}/\text{nm}$ ($\epsilon/\text{M}^{-1} \text{cm}^{-1}$) ^[a]	273 (4200)	273 (5500)
τ (H_2O)/ms	0.924(2)	2.50(1)
τ (D_2O)/ms	1.474(2)	2.99(1)
Δk_{obs}	0.404	0.07
$\Phi(\text{H}_2\text{O})$ (%) ^a	0.13	2.5
q	0.2 ^b	0.1 ^c
	0.1 ^d	

^a Absolute quantum yields measured relative to quinine sulfate in diluted acidic solution (absolute quantum yield: 0.546).³² ^b eqn (3). ^c eqn (4). ^d eqn (5).

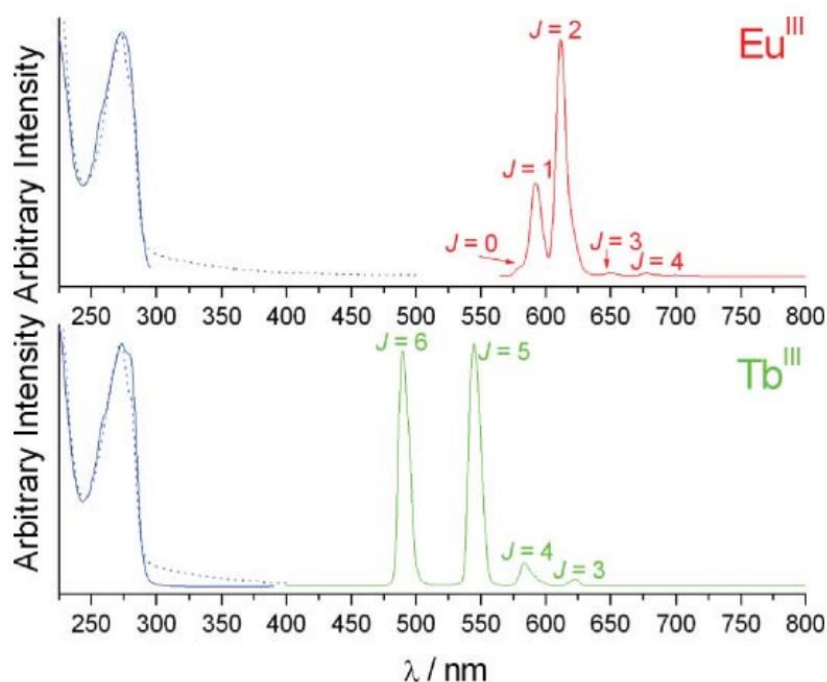


Fig. 2. Absorption (dotted blue lines), excitation (solid blue lines) and emission spectra of $[\text{Ln}(\text{bp15c5})]^+$ complexes ($\text{Ln} = \text{Eu}$ or Tb) as recorded from 10^{-5} M aqueous solutions at pH 7.0.

The number of inner sphere water molecules (q) can be determined by using luminescence lifetime measurements on solutions of Eu^{III} or Tb^{III} complexes in H_2O and D_2O .^{36,37} This method is based on the fact that O–H oscillators of coordinated water molecules quench the Ln^{III} excited state more efficiently than O–D oscillators of D_2O . Considering that the most common coordination numbers for Ln^{III} complexes in solution are 8 and 9, as well as the nonadentate nature of the bp15c5 ligand, one would expect the $[\text{Ln}(\text{bp15c5})]^+$ systems to exist in solution as $q = 0$ complexes. However, several examples of ten-coordinated Ln^{III} complexes in aqueous solution have been reported in the literature,^{38,39} including the $[\text{Eu}(\text{bp12c4})(\text{H}_2\text{O})_2]^+$ complex.²³ Therefore, the presence of one inner-sphere water molecule for the $[\text{Ln}(\text{bp15c5})]^+$ complexes should be considered.

The emission lifetimes of the $\text{Tb}({}^5\text{D}_4)$ and $\text{Eu}({}^5\text{D}_0)$ excited levels of $[\text{Ln}(\text{bp15c5})]^+$ complexes were measured in 10^{-5} M D_2O and H_2O solutions of the complexes, and used to calculate the number of coordinated water molecules q according to the method proposed by Parker and co. [eqn (3) and (4)].⁴⁰

$$q_{\text{Eu}} = 1.2(\Delta k_{\text{obs}} - 0.25) \quad (3)$$

$$q_{\text{Tb}} = 5.0(\Delta k_{\text{obs}} - 0.06) \quad (4)$$

In these equations $\Delta k_{\text{obs}} = k_{\text{obs}}(\text{H}_2\text{O}) - k_{\text{obs}}(\text{D}_2\text{O})$ and $k_{\text{obs}} = 1/\tau_{\text{obs}}$. These calculations provide q values of 0.2 (Eu^{III}) and 0.1 (Tb^{III}). The use of the expression proposed by Horrocks *et al.*⁴¹ for Eu^{III} complexes [eqn (5)] provides a similar result (Table 2), with an estimated uncertainty for q of ± 0.1 .

$$q_{\text{Eu}} = 1.11(\Delta k_{\text{obs}} - 0.31) \quad (5)$$

These results indicate the absence of inner-sphere water molecules in the $[\text{Ln}(\text{bp15c5})]^+$ complexes, which probably results in nine-coordinate complexes.

${}^1\text{H}$ and ${}^{13}\text{C}$ NMR spectra

The ${}^1\text{H}$ and ${}^{13}\text{C}$ NMR spectra of the diamagnetic $[\text{Ln}(\text{bp15c5})]^+$ complexes ($\text{Ln} = \text{La}$ or Lu) were recorded in D_2O solution at $\text{pD} = 7.0$ (Fig. 3). The spectra of both complexes are very similar, suggesting that they adopt similar structures in aqueous solution (Fig. S1, ESI[†]). The spectra of the La^{III} analogue were assigned with the aid of HSQC and HMBC 2D heteronuclear experiments as well as standard 2D homonuclear COSY and NOESY experiments (Table 3). The two picolate pendant arms are magnetically non-equivalent, which results in a C_1 symmetry of the complex in solution. This is confirmed by the ${}^{13}\text{C}$ NMR spectrum, which shows 24 signals for the 24 carbon nuclei of the ligand backbone. The signals due to protons H7a, H7b, H18a and H18b show AB spin patterns where the larger shifts for H7b and H18b result from the combined deshielding effects of the pyridyl ring current and the polarizing effect of the Ln^{III} ion on the C–H bond pointing away from it (Fig. 3).⁴² These results indicate a slow interconversion between the Δ and Λ optical isomers arising from the different orientation of the two pendant arms (see below). The axial and equatorial protons of the macrocyclic fragment are magnetically non-equivalent. This indicates that the interconversion between the δ and λ conformations of the five-membered quelate rings formed upon

coordination of the crown moiety is slow in the NMR time-scale, pointing to a relatively rigid structure of the crown moiety in solution. This is compatible with a nonadentate binding of the macrocyclic ligand to the Ln^{III} ions.

Table 3. ¹H and ¹³C NMR Shifts (ppm with respect to TMS) of [La(bp15c5)]⁺ recorded in D₂O solution (pD = 7.0) at 298 K. See Scheme 2 for labelling^a.

H3	8.03	H13ax	3.68	C1	173.3	C16	68.9
H4	8.14	H13eq	2.91	C2	150.6	C17	55.1
H5	7.70	H14ax	3.45	C3	123.8	C18	63.4
H7a	3.97	H14eq	2.61	C4	140.8	C19	158.6
H7b	4.52	H15ax	3.70	C5	125.8	C20	124.6
H8ax	2.72	H15eq	3.45	C6	157.7	C21	141.1
H8eq	3.12	H16ax	3.96	C7	64.2	C22	123.5
H9ax	3.74	H16eq	3.13	C8	54.4	C23	149.1
H9eq	3.21	H17ax	2.74	C9	71.2	C24	173.1
H10ax	3.60	H17eq	2.74	C10	69.6		
H10eq	3.91	H18a	4.16	C11	69.6		
H11ax	3.81	H18b	4.40	C12	68.1		
H11eq	4.18	H20	7.73	C13	55.8		
H12ax	4.15	H21	8.13	C14	53.0		
H12eq	4.15	H22	8.07	C15	68.8		

$$a^2 J_{18a-18b} = 16.8 \text{ Hz}; {}^2J_{7a-7b} = 15.4 \text{ Hz}.$$

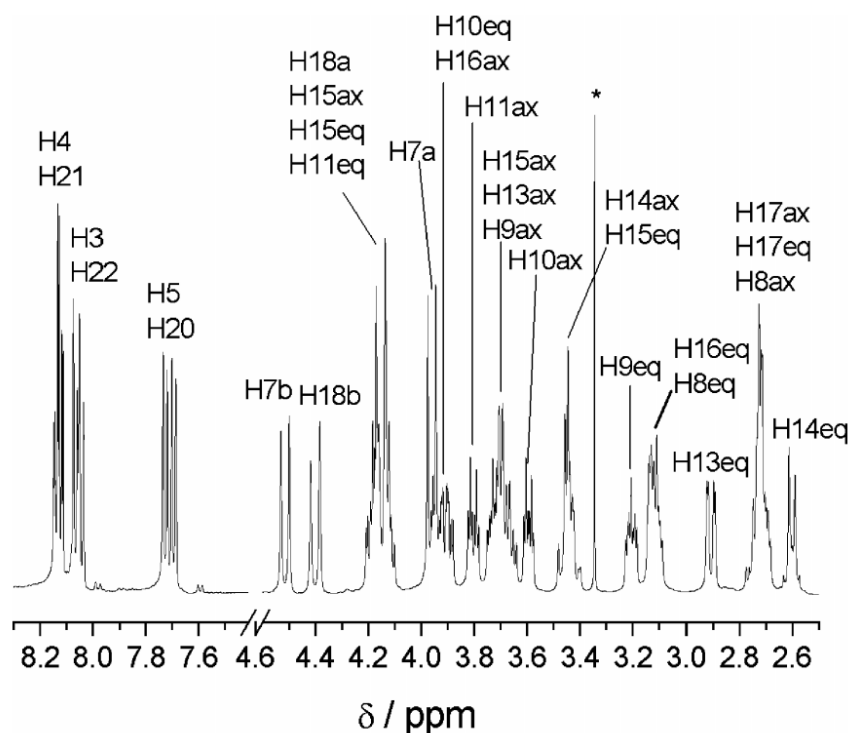
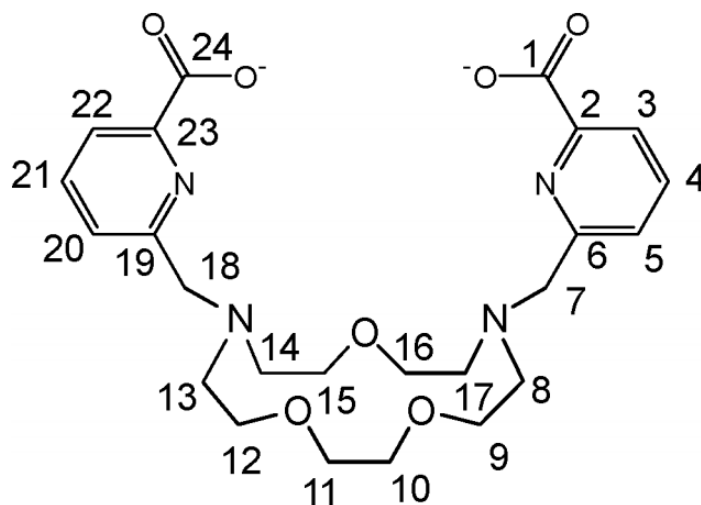


Fig. 3. ¹H NMR spectrum (500 MHz) of [La(bp15c5)]⁺ recorded in D₂O solution (pD = 7.0) at 298 K. The asterisk denotes MeOH coming from the ligand synthesis. See Scheme 2 for labelling.

The specific CH₂ proton assignments of the axial and equatorial H7–H18 protons were not possible on the basis of the 2D NMR spectra. However, it is known from previous ¹H NMR studies on Ln^{III} complexes with macrocyclic ligands that the ring axial protons experience strong coupling with the geminal protons and the vicinal axial protons, while the equatorial protons provide strong coupling with the geminal protons only.⁴³ Indeed, the ³J_{H-H} coupling constants characterising the coupling between vicinal pairs of protons (axial–axial, axial–equatorial and equatorial–equatorial) follow the *Karplus* equation [³J_{H-H} = 7-cosϕ+5cos2ϕ, where ϕ represents the H–C–C–H dihedral angle].⁴⁴ According to our DFT calculations (see below), the ϕ values involving axial–axial vicinal protons are close to 180° (171–178°), while the dihedral angles defined by axial–equatorial and equatorial–equatorial vicinal protons fall within the range 43–77°. Thus, the specific assignment of the axial and equatorial protons could be achieved in some cases by observing the coupling pattern of the proton signals. For instance, the signals due to protons H14 and H13 observed at 2.61 and 2.91 ppm (Fig. 3), could be assigned to equatorial protons, as the spin coupling pattern is dominated by a ²J_{H-H} of 12–13 Hz, the ³J_{H-H} values being substantially smaller (< 4 Hz). In other cases the assignments of the equatorial and axial protons could be achieved by observing the cross-peaks in the COSY spectra, as axial protons are expected to give two strong cross-peaks (geminal and axial–axial), whereas equatorial protons should show one strong (geminal) and two weak (equatorial–equatorial and equatorial–axial) cross-peaks.

The ¹H NMR spectra of the paramagnetic Ce^{III}, Eu^{III} and Yb^{III} complexes were also obtained in D₂O solution. The proton spectra consist of 30 signals, which again points to a C₁ symmetry of the complexes in solution (Fig. 4). The binding of a ligand to a paramagnetic Ln^{III} ion generally results in large NMR frequency shifts at the ligand nuclei, with magnitudes and signs depending critically on both the nature of the lanthanide ion and the location of the nucleus relative to the metal centre.⁴⁵ This is indeed the case of the paramagnetic [Ln(bp15c5)]⁺ complexes (Fig. 4), for which the ¹H NMR signals are observed in the range 16 to –8 (Ce^{III}), 19 to –18 (Eu^{III}) and 70 to –45 ppm (Yb^{III}). The 24 ¹H NMR signals due to protons 7–18 (Scheme 2) can be grouped into two different sets according to their relative line broadening, 12 resonances being appreciably sharper than the remaining ones (Fig. 4). These two sets of signals correspond to two sets of Ln^{III}-proton distances, the broader resonances being associated to the axial protons, which are closer to the metal ion.⁴⁶ Unfortunately, an assignment of the spectra was not possible due to the large number of proton signals and the low symmetry of the complex. However, the spectra confirm a nonadentate coordination of the ligand to the metal ions in aqueous solution.



Scheme 2. Ligand bp15c5²⁻ and its labelling scheme used for NMR spectral assignment.

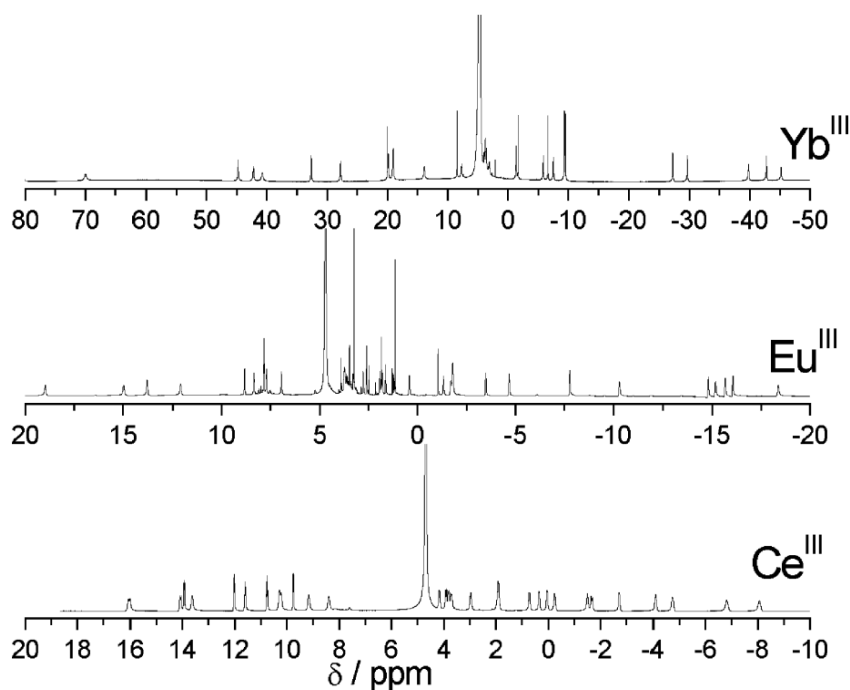


Fig. 4. ^1H NMR spectra (300 MHz) of $[\text{Ln}(\text{bp}15\text{c}5)]^+$ complexes ($\text{Ln} = \text{Ce}, \text{Eu}$ or Yb) recorded in D_2O solution ($\text{pD} = 7.0$) at 298 K.

DFT calculations

Aiming to obtain information about the structure in solution of the $[\text{Ln}(\text{bp}15\text{c}5)]^+$ complexes we have performed DFT calculations based on the B3LYP model. On the grounds of our previous experience,^{47,48} in these calculations we have used the effective core potential (ECP) of Dolg *et al.*⁴⁹ and the related [5s4p3d]-GTO valence basis set for the lanthanides, while the remaining atoms were described by using the 6-31G(d) basis set. This ECP includes 46+4 f^{el} electrons in the core, leaving the outermost 11 electrons to be treated explicitly.

In our previous papers we have shown that in the $[\text{Ln}(\text{bp}12\text{c}4)]^+$ and $[\text{Ln}(\text{bp}18\text{c}6)]^+$ complexes the ligand adopts a *syn* conformation, with the two pendant arms being oriented to the same side of the macrocyclic fragment.^{21,23} Furthermore, previous investigations on Ln^{III} complexes derived from 1,10-diaza-15-crown-5 containing coordinating pendant arms have also revealed a *syn* conformation of the ligand in the corresponding complexes.⁵⁰ Thus, it is reasonable to assume that the complexes of bp15c5 will adopt a similar structure. A *syn* conformation of the ligand in $[\text{Ln}(\text{bp}15\text{c}5)]^+$ complexes implies the occurrence of two helicities: one associated with the layout of the picolinate pendant arms (absolute configuration Δ or Λ), and the other to the five five-membered chelate rings formed by the binding of the crown moiety (each of them showing absolute configuration δ or λ).^{51,52} A detailed analysis of the coordinative properties of the bp15c5 ligand indicates that there are up to 64 possible conformations (32 enantiomeric pairs of diastereoisomers) of the complexes of this ligand combining different helicities of the pendant arms and the five-membered rings formed upon coordination of the crown moiety.²⁵ Thus, in order to reduce the computational cost of the conformational analysis, we initially investigated the conformational space at the HF/3-21G level by performing full geometry optimizations of the 32 diastereoisomeric forms of the complexes with the ligand adopting a *syn* conformation. The ten most stable conformations for each complex were then fully optimized at the B3LYP/6-31G(d) level. Full geometry optimization of each conformation performed *in vacuo* was followed by single point energy calculations in aqueous solution (C-PCM model).

The minimum energy conformation obtained from our calculations for all Ln^{III} ions investigated corresponds to the $\Lambda(\lambda\delta)(\delta\delta\lambda)$ form (Fig. 5). A second diastereoisomeric form, $\Lambda(\lambda\delta)(\delta\lambda\lambda)$, is close in energy to the former one, particularly for the large lanthanides; the energy difference between these two forms amounts only to 0.85 kJ mol⁻¹ for La^{III}, and it increases to 4.10 kJ mol⁻¹ for Lu^{III}. The remaining conformations investigated show high relative energies with respect to the minimum energy conformation (8.3–37.8 kJ mol⁻¹). The relative energies of most of conformations investigated show a smooth change along the lanthanide series from La^{III} to Lu^{III}. However, two conformations [$\Lambda(\delta\delta)(\delta\delta\delta)$ and $\Lambda(\lambda\delta)(\delta\delta\delta)$, Fig. 5] show an abrupt destabilization upon decreasing the ionic radius of the Ln^{III} ion from Eu^{III} to Ho^{III}, and then become more stable for Lu^{III}. This abrupt change in the energetic trend from Eu^{III} to Ho^{III} is due to the decoordination of one of the oxygen atoms of the crown moiety [O(5), Fig. 6], leading to eight-coordinate complexes. This result is in line with a better fit of the crown moiety size of the ligand and the large Ln^{III} ions.

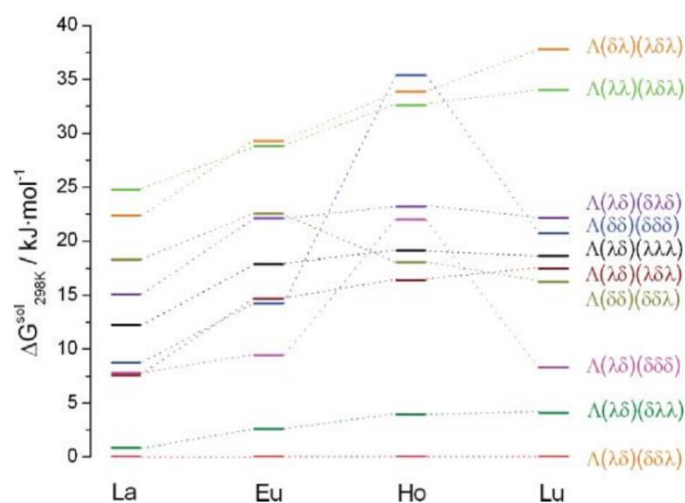


Fig. 5. C-PCM relative free energies of different diastereoisomeric forms of $[\text{Ln}(\text{bp}15\text{c}5)]^+$ complexes (Ln = La, Eu, Ho or Lu) in aqueous solution.

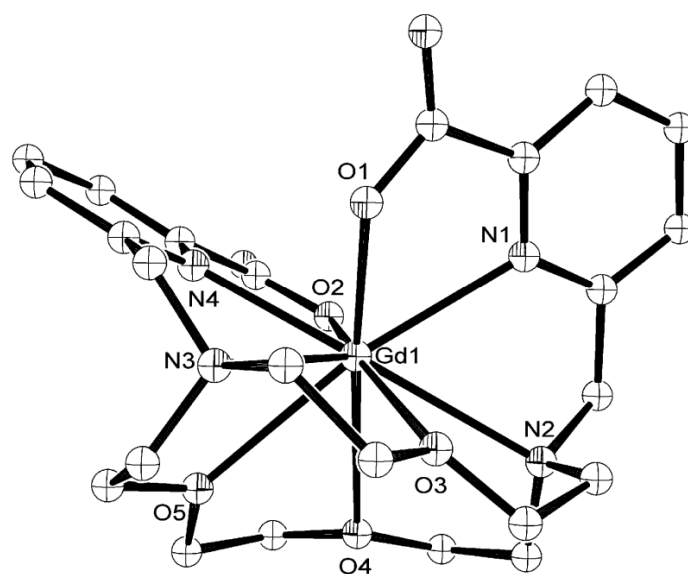


Fig. 6. Minimum energy conformation of the $[\text{Gd}(\text{bp}15\text{c}5)]^+$ complex obtained from DFT calculations. Hydrogen atoms are omitted for simplicity.

In a recent paper we have shown that our computational procedure provides relative free energies of Ln^{III} DOTA-like complexes that deviate from the experimental values by 0.8–4.6 kJ mol⁻¹.⁴⁸ Furthermore, a single species in solution is observed in the NMR spectra of the [Ln(bp15c5)]⁺ complexes (Ln = La, Ce, Eu, Yb or Lu). Thus, we may conclude that most likely the [Ln(bp15c5)]⁺ complexes adopt a $\Lambda(\lambda\delta)(\delta\delta\lambda)$ conformation in aqueous solution.

Table 4 shows the bond distances of the metal coordination environment calculated for the $\Lambda(\lambda\delta)(\delta\delta\lambda)$ conformation of [Ln(bp15c5)]⁺ complexes, while the optimized geometry of the Gd^{III} complex is shown in Fig. 6. Most of the distances between the Ln^{III} ions and the donor atoms of the ligand decrease along the lanthanide series, as usually observed for Ln^{III} complexes as a consequence of the lanthanide contraction.¹ However, the distances between the Ln^{III} ion and two of the oxygen atoms of the crown moiety [O(4) and O(5)] follow a different trend. Indeed, these distances decrease along the series from La^{III} to Gd^{III}, and then increase for the smaller Ho^{III} and Lu^{III} ions. Thus, the interaction between the Ln^{III} ion and several of the donor atoms of bp15c5 is weakened as the ionic radius of the metal ion decreases. These results clearly indicate a better match between the binding sites offered by the ligand structure and the binding sites required by large Ln^{III} ions, which results in a drop of the complex stability upon decreasing the ionic radius of the metal ion.

In a previous paper we have reported the X-ray single structure of the [Cd(bp15c5)] complex,²⁵ where the metal ion is seven-coordinate. Interestingly, in [Cd(bp15c5)] the two donor atoms of the ligand that remain uncoordinated correspond to those for which a lengthening of the Ln-donor distances is predicted by our DFT calculations [O(4) and O(5)]. Thus, the lengthening of the distances between the metal ion and these donor atoms appears to be a general strategy adopted by bp15c5 to accommodate small metal ions.

Table 4. Bond distances [Å] of the metal coordination environments obtained for the $\Lambda(\lambda\delta)(\delta\delta\lambda)$ conformation of [Ln(bp15c5)]⁺ complexes at the B3LYP/6-31G(d) level^a.

	La	Nd	Gd	Ho	Lu
Ln(1)–O(1)	2.398	2.343	2.285	2.245	2.192
Ln(1)–O(2)	2.371	2.314	2.253	2.213	2.165
Ln(1)–O(3)	2.657	2.599	2.534	2.490	2.436
Ln(1)–O(4)	2.843	2.825	2.821	2.839	2.902
Ln(1)–O(5)	2.777	2.753	2.737	2.743	2.771
Ln(1)–N(1)	2.717	2.668	2.614	2.577	2.532
Ln(1)–N(2)	2.976	2.936	2.894	2.866	2.840
Ln(1)–N(3)	2.819	2.780	2.737	2.714	2.686
Ln(1)–N(4)	2.630	2.570	2.508	2.466	2.415

^a Geometry optimizations were performed in the gas-phase. See Fig. 6 for labelling.

Conclusions

The dianionic nonadentate bp15c5 receptor forms moderately stable complexes with the Ln^{III} ions in aqueous solution. The stability constants determined for the [Ln(bp15c5)]⁺ complexes are considerably lower than those of the analogues derived from bp12c4, but close to those of [Ln(bp18c6)]⁺ complexes, particularly for the heaviest Ln^{III} ions. The bp15c5 ligand provides a nonadentate binding to the Ln^{III} ions along the whole lanthanide series from La^{III} to Lu^{III}, resulting in $q = 0$ complexes. This is in contrast with the situation observed for the [Ln(bp12c4)]⁺ complexes, for which an equilibrium between $q = 1$ and $q = 2$ species exists

around the middle of the lanthanide series. The drop of stability in $[\text{Ln}(\text{bp15c5})]^+$ complexes upon decreasing the ionic radius of the metal ion is attributed to the better match between the binding sites offered by the ligand structure and the binding sites required by large Ln^{III} ions.

Experimental section

Solvents and starting materials

N,N'-Bis[(6-carboxy-2-pyridyl)methylene]-1,10-diaza-15-crown-5 ($\text{H}_2\text{bp15c5}$) was prepared as previously reported by us.²⁵ All other chemicals were purchased from commercial sources and used without further purification, unless otherwise stated.

Physical methods

^1H and ^{13}C NMR spectra were recorded at 25 °C on Bruker Avance 300 and Bruker Avance 500 MHz spectrometers. For measurements in D_2O , *tert*-butyl alcohol was used as an internal standard with the methyl signal calibrated at $\delta = 1.2$ (^1H) and 31.2 ppm (^{13}C). Spectral assignments were based in part on two-dimensional NOESY, COSY, HMQC, and HMBC experiments. Electronic spectra in the UV-Vis range were recorded at 25 °C on a Perkin–Elmer Lambda 900 UV-Vis spectrophotometer using 1.0 cm quartz cells. Excitation and emission spectra were recorded on a Perkin–Elmer LS-50B spectrometer. Luminescence lifetimes were calculated from the monoexponential fitting of the average decay data, and they are averages of at least 3–5 independent determinations. Quantum yields of the metal centred luminescence were measured relative to quinine sulfate in diluted acidic solution (absolute quantum yield: 0.546).³²

Potentiometric measurements

The stock solutions of LnCl_3 were prepared from $\text{LnCl}_3 \cdot x\text{H}_2\text{O}$. The concentration of the solutions was determined by complexometric titration with a standardized $\text{Na}_2\text{H}_2\text{EDTA}$ solution (H_4EDTA = ethylenediaminetetraacetic acid) using xylenol orange as indicator. Ligand stock solutions were prepared in double distilled water and the exact ligand concentration was determined from the potentiometric titration curves with KOH.

Ligand protonation constants and stability constants of Ln^{III} complexes were determined by pH-potentiometric titration at 25 °C in 0.1 M KCl. As observed for bp18c6 and bp12c4,^{21,22} the stability constants could be determined from direct potentiometric titrations, as complex formation was fast. The samples (3–5 ml) were stirred while a constant N_2 flow was bubbled through the solutions. The pH of the titration mixture was adjusted by addition of a known volume of standard aqueous HCl. The titrations were carried out adding standardized KOH solution with a Metrohm 702 SM Titrino automatic burette. A Metrohm 692 pH/ion-meter was used to measure pH. The H^+ concentration was obtained from the measured pH values using the correction method proposed by Irving *et al.*⁵³ The ligand and metal–ligand (1 : 1) solutions (3.5 mM) were titrated over the pH range $2.0 < \text{pH} < 12.0$. The titration data for Ln^{III} complexation were successfully refined assuming the presence of only 1 : 1 metal–ligand species in solution; in all cases only data corresponding to the lower portions of the titration curves were employed for the calculations in order to avoid complications arising from competing hydrolysis/precipitation at higher pH values. The protonation and stability constants were calculated from parallel titrations with the program PSEQUAD.⁵⁴ The errors given correspond to one standard deviation.

Computational methods

All calculations were performed with the Gaussian 03 package (Revision C.01).⁵⁵ Full geometry optimizations of the $[\text{Ln}(\text{bp15c5})]^+$ ($\text{Ln} = \text{La}, \text{Ce}, \text{Pr}, \text{Nd}, \text{Eu}, \text{Gd}, \text{Ho}, \text{Yb}$ or Lu) systems were performed *in*

vacuo at the HF level by using the effective core potential (ECP) of Dolg *et al.* and the related [5s4p3d]-GTO valence basis set for the lanthanides,⁴⁹ and the 3-21G basis set for C, H, N and O atoms. The ten most stable conformations obtained from HF calculations were then fully optimized employing hybrid DFT with the B3LYP exchange–correlation functional^{56,57} and the 6-31G(d) basis set for the ligand atoms. In aqueous solution relative free energies of the different isomers were calculated from solvated single point energy calculations on the geometries optimized *in vacuo*. Solvent effects were evaluated by using the polarizable continuum model (PCM). In particular, we used the C-PCM variant⁵⁸ that employs conductor rather than dielectric boundary conditions. The solute cavity is built as an envelope of spheres centered on atoms or atomic groups with appropriate radii. Calculations were performed using an average area of 0.2 Å² for all the finite elements (tesserae) used to build the solute cavities. For lanthanides the previously parameterized radii were used.⁵⁹ Final free energies include both electrostatic and nonelectrostatic contributions.

Acknowledgements

The authors thank Ministerio de Educación y Ciencia (MEC) and Fondo Europeo de Desarrollo Regional (FEDER) (CTQ2006-07875 and CTQ2009-10721), and Xunta de Galicia (INCITE09E1R103013ES) for financial support. The authors are indebted to Centro de Supercomputación de Galicia (CESGA) for providing the computer facilities.

Notes and references

1. M. Seitz, A. G. Oliver and K. Raymond, *J. Am. Chem. Soc.*, 2007, **129**, 11153–11160.
2. R. D. Shannon, *Acta Crystallogr., Sect. A: Cryst. Phys., Diffr., Theor. Gen. Crystallogr.*, 1976, **A32**, 751–767.
3. K. L. Nash and M. P. Jensen, In *Handbook on the Physics and Chemistry of Rare Earths*. J. K. A. Gschneidner and L. Eyring, (ed.), (Elsevier, Amsterdam, 2000, **28**, 311–371.
4. N. André, R. Scopelliti, G. Hopfgartner, C. Piguet and J.-C. G. Bünzli, *Chem. Commun.*, 2002, 214–215; C. Piguet and J.-C. G. Bünzli, *Chem. Soc. Rev.*, 1999, **28**, 347–358; S. Floquet, M. Borkovec, G. Bernardinelli, A. Pinto, L.-A. Leuthold, G. Hopfgartner, D. Imbert, J.-C. G. Bünzli and C. Piguet, *Chem.–Eur. J.*, 2004, **10**, 1091–1105.
5. G. R. Choppin, *J. Alloys Compd.*, 1997, **249**, 1–8.
6. S. A. Cotton, *C. R. Chimie*, 2008, **8**, 129–145.
7. P. Caravan, J. J. Ellison, T. J. McMurphy and R. B. Lauffer, *Chem. Rev.*, 1999, **99**, 2293–2352.
8. G. Tircso, E. T. Benyo, E. H. Suh, P. Jurek, G. E. Kiefer, A. D. Sherry and Z. Kovacs, *Bioconjugate Chem.*, 2009, **20**, 565–575; G. Tircso, Z. Kovacs and A. D. Sherry, *Inorg. Chem.*, 2006, **45**, 9269–9280; W. D. Kim, D. C. Hrcir, G. E. Kiefer and A. D. Sherry, *Inorg. Chem.*, 1995, **34**, 2225–2232; W. D. Kim, G. E. Kiefer, F. Maton, K. McMillan, R. N. Muller and A. D. Sherry, *Inorg. Chem.*, 1995, **34**, 2233–2243; S. W. Bligh, N. Choi, C. F. G. C. Geraldès, S. Knoke, M. McPartlin, M. J. Sanganee and T. M. Woodroffe, *J. Chem. Soc., Dalton Trans.*, 1997, 4119–4126; S. Aime, C. Cavallotti, E. Gianolio, G. B. Giovenzana, G. Palmisano and M. Sisti, *Org. Lett.*, 2004, **6**, 1201–1204; S. Aime, E. Gianolio, D. Corpillo, C. Cavallotti, G. Palmisano, M. Sisti, G. B. Giovenzana and R. Pagliarin, *Helv. Chim. Acta*, 2003, **86**, 615–632; S. Aime, M. Botta, L. Frullano, S. G. Crich, G.

- Giovenzana, R. Pagliarin, G. Palmisano, F. R. Sirtori and M. Sisti, *J. Med. Chem.*, 2000, **43**, 4017–4024; R. Delgado, J. Costa, K. P. Guerra and L. M. P. Lima, *Pure Appl. Chem.*, 2005, **77**, 569–579; F. Marques, K. P. Guerra, L. Gano, J. Costa, M. P. Campello, L. M. P. Lima, R. Delgado and I. Santos, *JBIC, J. Biol. Inorg. Chem.*, 2004, **9**, 859–872; Q. Zheng, H. Dai, M. E. Merritt, C. Malloy, C. Y. Pan and W.-H. Li, *J. Am. Chem. Soc.*, 2005, **127**, 16178–16188.
9. S. Aime, A. S. Batsanov, M. Botta, J. A. K. Howard, M. P. Lowe and D. Parker, *New J. Chem.*, 1999, **23**, 669–670; M. Polasek, M. Sedinova, J. Kotek, L. Vander Elst, R. N. Muller, P. Hermann and I. Lukes, *Inorg. Chem.*, 2009, **48**, 455–465; M. Polasek, J. Kotek, P. Hermann, I. Cisarova, K. Binnemans and I. Lukes, *Inorg. Chem.*, 2009, **48**, 466–475.
 10. N. Weibel, L. Charbonniere and R. Ziessel, *Tetrahedron Lett.*, 2006, **47**, 1793–1796; A. Borel, H. Kang, C. Gateau, M. Mazzanti, R. B. Clarkson and R. L. Belford, *J. Phys. Chem. A*, 2006, **110**, 12434–12438; P. H. Fries, C. Gateau and M. Mazzanti, *J. Am. Chem. Soc.*, 2005, **127**, 15801–15814; C. Gateau, M. Mazzanti, J. Pecaut, F. A. Dunand and L. Helm, *Dalton Trans.*, 2003, 2428–2433; Y. Bretonniere, M. Mazzanti, J. Pecaut, F. A. Dunand and A. E. Merbach, *Chem. Commun.*, 2001, 621–622; Y. Bretonniere, M. Mazzanti, J. Pecaut, F. A. Dunand and A. E. Merbach, *Inorg. Chem.*, 2001, **40**, 6737–6745; A. Nonat, P. H. Fries, J. Pecaut and M. Mazzanti, *Chem.–Eur. J.*, 2007, **13**, 8489–8506; A. Nonat, M. Giraud, C. Gateau, P. H. Fries, L. Helm and M. Mazzanti, *Dalton Trans.*, 2009, 8033–8046; M. Mato-Iglesias, C. Platas-Iglesias, K. Djanashvili, J. A. Peters, E. Tóth, E. Balogh, R. N. Muller, L. Vander Elst, A. de Blas and T. Rodríguez-Blas, *Chem. Commun.*, 2005, 4729–4731; E. Balogh, M. Mato-Iglesias, C. Platas-Iglesias, E. Tóth, K. Djanashvili, J. A. Peters, A. de Blas and T. Rodríguez-Blas, *Inorg. Chem.*, 2006, **45**, 8719–8728.
 11. C. Platas-Iglesias, M. Mato-Iglesias, K. Djanashvili, R. N. Muller, L. Vander Elst, J. A. Peters, A. de Blas and T. Rodríguez-Blas, *Chem.–Eur. J.*, 2004, **10**, 3579–3590; N. Chatterton, Y. Bretonniere, J. Pecaut and M. Mazzanti, *Angew. Chem., Int. Ed.*, 2005, **44**, 7595–7598.
 12. P. Caravan, T. Hedlund, S. Liu, S. Sjöberg and C. Orvig, *J. Am. Chem. Soc.*, 1995, **117**, 11230–11238; D. Chapon, J.-P. Morel, P. Delangle, C. Gateau and J. Pécaut, *Dalton Trans.*, 2003, 2745–2749.
 13. L. Sarka, I. Bányai, E. Brücher, R. Király, J. Platzek, B. Radüchel and H. Schmitt-Willich, *J. Chem. Soc., Dalton Trans.*, 2000, 3699–3703.
 14. M. Mato-Iglesias, T. Rodriguez-Blas, C. Platas-Iglesias, M. Starck, P. Kadjane, R. Ziessel and L. Charbonniere, *Inorg. Chem.*, 2009, **48**, 1507–1518.
 15. C. A. Chang and M. E. Rowland, *Inorg. Chem.*, 1983, **22**, 3866–3869.
 16. L. Tei, Z. Baranyai, E. Brucher, C. Cassino, F. Demicheli, N. Masciocchi, G. B. Giovenzana and M. Botta, *Inorg. Chem.*, 2010, **49**, 616–625.
 17. R. D. Hancock and A. E. Martell, *Chem. Rev.*, 1989, **89**, 1875–1914; R. D. Hancock and A. E. Martell, *Supramol. Chem.*, 1996, **6**, 401–407; B. P. Hay and R. D. Hancock, *Coord. Chem. Rev.*, 2001, **212**, 61–78.
 18. R. D. Hancock, H. Maumela and A. S. de Sousa, *Coord. Chem. Rev.*, 1996, **148**, 315–317.
 19. Y. Inoue and G. W. Gokel, in *Cation Binding by Macrocycles. Complexation of Cationic Species by Crown Ethers*, Marcel Dekker, New York, 1990.
 20. R. M. Izatt, K. Pawlak, J. S. Bradshaw and R. L. Bruening, *Chem. Rev.*, 1991, **91**, 1721–1785; R. M. Izatt, J. S. Bradshaw, K. Pawlak, R. L. Bruening and B. J. Tarbet, *Chem. Rev.*, 1992, **92**, 1261–1354;

- G. W. Gokel, *Chem. Soc. Rev.*, 1992, **21**, 39–47; R. M. Izatt, K. Pawlak and J. S. Bradshaw, *Chem. Rev.*, 1995, **95**, 2529–2586.
21. A. Roca-Sabio, M. Mato-Iglesias, D. Esteban-Gomez, E. Toth, A. de Blas, C. Platas-Iglesias and T. Rodríguez-Blas, *J. Am. Chem. Soc.*, 2009, **131**, 3331–3341.
 22. Z. Palinkas, A. Roca-Sabio, M. Mato-Iglesias, D. Esteban-Gomez, C. Platas-Iglesias, A. de Blas, T. Rodriguez-Blas and E. Toth, *Inorg. Chem.*, 2009, **48**, 8878–8889.
 23. M. Mato-Iglesias, A. Roca-Sabio, Z. Palinkas, D. Esteban-Gomez, C. Platas-Iglesias, E. Toth, A. de Blas and T. Rodriguez-Blas, *Inorg. Chem.*, 2008, **47**, 7840–7851.
 24. C. A. Chang and V. O. Ochaya, *Inorg. Chem.*, 1986, **25**, 355–358.
 25. R. Ferreirós-Martínez, C. Platas-Iglesias, A. de Blas, D. Esteban-Gómez and T. Rodríguez-Blas, *Eur. J. Inorg. Chem.*, 2010, 2495–2503.
 26. P. Mateus, N. Bernier and R. Delgado, *Coord. Chem. Rev.*, 2010, **254**, 1726–1747.
 27. N. Chatterton, C. Gateau, M. Mazzanti, J. Pecaut, A. Borel, L. Helm and A. E. Merbach, *Dalton Trans.*, 2005, 1129–1135.
 28. R. Ferreiros-Martinez, D. Esteban-Gomez, C. Platas-Iglesias, A. de Blas and T. Rodriguez-Blas, *Dalton Trans.*, 2008, 5754–5765.
 29. M. Mato-Iglesias, E. Balogh, C. Platas-Iglesias, E. Toth, A. de Blas and T. Rodríguez-Blas, *Dalton Trans.*, 2006, 5404–5415.
 30. R. Ferreiros-Martinez, D. Esteban-Gómez, C. Platas-Iglesias, A. de Blas and T. Rodríguez-Blas, *Inorg. Chem.*, 2009, **48**, 10976–10987.
 31. A. E. Martell, R. J. Motekaitis, R. M. Smith, *NIST Critically selected stability constants of metal complexes database*. Version 8.0 for windows. Gaithersburg, MD: National Institute of Standards and Technology, Standard Reference Data Program, 2004.
 32. S. R. Meech and D. Phillips, *J. Photochem.*, 1983, **23**, 193–217.
 33. L. J. Charbonniere, N. Weibel, P. Retailleau and R. Ziessel, *Chem.–Eur. J.*, 2007, **13**, 346–358.
 34. N. Sabbatini, M. Guardigli and J.-M. Lehn, *Coord. Chem. Rev.*, 1993, **123**, 201–228; S. I. Weissmann, *J. Chem. Phys.*, 1942, **10**, 214–217.
 35. A.-S. Chauvin, F. Gumy, D. Imbert and J.-C. G. Bünzli, *Spectrosc. Lett.*, 2004, **37**, 517–532; A.-S. Chauvin, F. Gumy, D. Imbert and J.-C. G. Bünzli, *Spectrosc. Lett.*, 2007, **40**, 193, *erratum*.
 36. W. D. Horrocks, Jr. and D. R. Sudnick, *Acc. Chem. Res.*, 1981, **14**, 384–392.
 37. W. D. Horrocks, Jr. and D. R. Sudnick, *J. Am. Chem. Soc.*, 1979, **101**, 334–340.
 38. L. Valencia, J. Martínez, A. Macías, R. Bastida, R. A. Carvalho and C. F. G. C. Geraldes, *Inorg. Chem.*, 2002, **41**, 5300–5312.
 39. M. del C. Fernández-Fernández, R. Bastida, A. Macías, P. Pérez-Lourido, C. Platas-Iglesias and L. Valencia, *Inorg. Chem.*, 2006, **45**, 4484–4496; C. Nuñez, R. Bastida, A. Macias, M. Mato-Iglesias, C. Platas-Iglesias and L. Valencia, *Dalton Trans.*, 2008, 3841–3850.

40. A. Beeby, I. M. Clarkson, R. S. Dickins, S. Faulkner, D. Parker, L. Royle, A. S. de Sousa, J. A. G. Williams and M. Woods, *J. Chem. Soc., Perkin Trans. 2*, 1999, 493–504.
41. R. M. Supkowski and E. D. Horrocks, Jr., *Inorg. Chim. Acta*, 2002, **340**, 44–48.
42. L. Vaiana, M. Regueiro-Figueroa, M. Mato-Iglesias, C. Platas-Iglesias, D. Esteban-Gómez, A. de Blas and T. Rodríguez-Blas, *Inorg. Chem.*, 2007, **46**, 8271–8282.
43. S. Aime, M. Botta and G. Ermondi, *Inorg. Chem.*, 1992, **31**, 4291–4299.
44. M. Karplus, *J. Am. Chem. Soc.*, 1963, **85**, 2870–2871; C. F. G. C. Geraldès, A. D. Sherry and G. E. Kiefer, *J. Magn. Reson.*, 1992, **97**, 290–304.
45. J. A. Peters, J. Huskens and D. J. Raber, *Prog. Nucl. Magn. Reson. Spectrosc.*, 1996, **28**, 283–350; I. Bertini, M. B. L. Janik, Y.-M. Lee, C. Luchinat and A. Rosato, *J. Am. Chem. Soc.*, 2001, **123**, 4181–4188.
46. S. Aime, L. Barbero, M. Botta and G. Ermondi, *J. Chem. Soc., Dalton Trans.*, 1992, 225–228.
47. M. Regueiro-Figueroa, D. Esteban-Gomez, A. de Blas, T. Rodriguez-Blas and C. Platas-Iglesias, *Eur. J. Inorg. Chem.*, 2010, 3586–3595; C. Nuñez, M. Mato-Iglesias, R. Bastida, A. Macías, P. Perez-Lourido, C. Platas-Iglesias and L. Valencia, *Eur. J. Inorg. Chem.*, 2009, 1086–1095.
48. M. Purgel, Z. Baranyai, A. de Blas, T. Rodríguez-Blas, I. Bányai, C. Platas-Iglesias and I. Tóth, *Inorg. Chem.*, 2010, **49**, 4370–4382.
49. M. Dolg, H. Stoll, A. Savin and H. Preuss, *Theor. Chim. Acta*, 1989, **75**, 173–194.
50. M. González-Lorenzo, C. Platas-Iglesias, F. Avecilla, C. F. G. C. Geraldès, D. Imbert, J.-C. G. Bünzli, A. de Blas and T. Rodríguez-Blas, *Inorg. Chem.*, 2003, **42**, 6946–6954.
51. E. J. Corey and J. C. Bailar, Jr., *J. Am. Chem. Soc.*, 1959, **81**, 2620–2629.
52. J. K. Beattie, *Acc. Chem. Res.*, 1971, **4**, 253–259.
53. H. M. Irving, M. G. Miles and L. Pettit, *Anal. Chim. Acta*, 1967, **38**, 475–488.
54. L. Zékány and I. Nagypál, In *Computation Methods for Determination of Formation Constants*, Ed. D. J. Leggett, Plenum, New York, 1985, p. 291.
55. *Gaussian 03*, Revision C.01, M. J. Frisch, G. W. Trucks, H. B. Schlegel, G. E. Scuseria, M. A. Robb, J. R. Cheeseman, J. A. Montgomery, Jr., T. Vreven, K. N. Kudin, J. C. Burant, J. M. Millam, S. S. Iyengar, J. Tomasi, V. Barone, B. Mennucci, M. Cossi, G. Scalmani, N. Rega, G. A. Petersson, H. Nakatsuji, M. Hada, M. Ehara, K. Toyota, R. Fukuda, J. Hasegawa, M. Ishida, T. Nakajima, Y. Honda, O. Kitao, H. Nakai, M. Klene, X. Li, J. E. Knox, H. P. Hratchian, J. B. Cross, V. Bakken, C. Adamo, J. Jaramillo, R. Gomperts, R. E. Stratmann, O. Yazyev, A. J. Austin, R. Cammi, C. Pomelli, J. W. Ochterski, P. Y. Ayala, K. Morokuma, G. A. Voth, P. Salvador, J. J. Dannenberg, V. G. Zakrzewski, S. Dapprich, A. D. Daniels, M. C. Strain, O. Farkas, D. K. Malick, A. D. Rabuck, K. Raghavachari, J. B. Foresman, J. V. Ortiz, Q. Cui, A. G. Baboul, S. Clifford, J. Cioslowski, B. B. Stefanov, G. Liu, A. Liashenko, P. Piskorz, I. Komaromi, R. L. Martin, D. J. Fox, T. Keith, M. A. Al-Laham, C. Y. Peng, A. Nanayakkara, M. Challacombe, P. M. W. Gill, B. Johnson, W. Chen, M. W. Wong, C. Gonzalez and J. A. Pople, Gaussian, Inc., Wallingford CT, 2004.
56. A. D. Becke, *J. Chem. Phys.*, 1993, **98**, 5648–5652.

57. C. Lee, W. Yang and R. G. Parr, *Phys. Rev. B*, 1988, **37**, 785–789.
58. V. Barone and M. Cossi, *J. Phys. Chem. A*, 1998, **102**, 1995–2001.
59. U. Cosentino, A. Villa, D. Pitea, G. Moro and V. Barone, *J. Phys. Chem. B*, 2000, **104**, 8001–8007.

† Electronic supplementary information (ESI) available: [NMR spectra](#) recorded for the La^{III} and Lu^{III} complexes of bp15c5, [¹H NMR](#) chemical shift data for the paramagnetic [Ln(bp15c5)]⁺ complexes (Ln = Ce^{III}, Eu^{III} or Yb^{III}), and optimized Cartesian coordinates of the [Ln(bp15c5)]⁺ complexes (B3LYP). See DOI: [10.1039/c0dt00746c](https://doi.org/10.1039/c0dt00746c).